The Atlantic Multidecadal Variability in a pre-industrial EC-Earth3 run

Bachelor's Degree in Science

Author
Stina Magndal

Supervisors
Moa Sporre
Annika Drews

Danmarks Meteorologiske Institut

LUND UNIVERSITY

Department of Physics
Division of Nuclear Physics

Duration: 2 months

Examination: May, 2023

Abstract

The Atlantic Multidecadal Variability (AMV) is a variation in sea surface temperature (SST) in the North Atlantic with a period of about 60-90 years. The drivers of this mode of variability are largely unknown as observational data only go back 150 years. Global climate models can help us better understand the AMV and its drivers and this thesis investigates how the AMV behaves in the Earth system model EC-Earth3. The thesis examines a 1000-year-long pre-industrial run and evaluates potential driving variables for the AMV. Specifically, the Atlantic Meridional Overturning Circulation (AMOC), which supplies the North Atlantic with warm, salty waters of tropical origin, as well as total cloud cover that affects the incoming solar radiation to the sea surface. The thesis finds that the AMOC is well correlated with the AMV with a lead of 4 years, suggesting that the AMOC is a key factor in modulating the AMV. It also finds that the AMV in the model experiences a period of around 128 years, longer than in observations, and that the subtropical arm of the AMV is weaker than in observations. Finally, the thesis finds positive cloud feedback in the subtropical arm of the AMV that enhance and propagate the changes in SSTs southward. Since the subtropical AMV arm is not as strong as in observations, the feedbacks are either not strong enough, or there are missing feedbacks needed to fully form the subtropical arm of the AMV in EC-Earth3.

Contents

List of Abbreviations

AMOC   Atlantic Meridional Overturning Circulation
AMV   Atlantic Multidecadal Variability
CGCM   Coupled General Circulation Model
CMIP6   Coupled Model Intercomparison Project phase 6
ESM   Earth System Model
GCM   Global Climate Model
NEMO   Nucleus for European Modelling of the Ocean
PSD   Power Spectrum Density
SLP   Sea Level Pressure
SST   Sea Surface Temperature
SSS   Sea Surface Salinity

1 Introduction

The North Atlantic undergoes a basin-scale variability in sea surface temperature (SST) with a period of between 60-90 years (Enfield et al., 2001; Schlesinger and Ramankutty, 1994). Formerly known as the Atlantic Multidecadal Oscillation (AMO), this mode of warming and cooling is now commonly referred to as the Atlantic Multidecadal Variability (AMV) due to the broad spectrum of low-frequency modes that signify it (Enfield et al., 2001; Knight et al., 2005; Schlesinger and Ramankutty, 1994; Sutton and Hodson, 2005; Zhang et al., 2019). Although the entire North Atlantic experiences warming (cooling) during the warm (cold) phase of the AMV, these changes in SST are strongest in the regions called the subpolar and subtropical arms of the AMV, seen in Fig. 1a. The subpolar arm has the strongest SST anomalies associated with it and is located in the western subpolar North Atlantic, just east of the Labrador sea. While the subtropical arm, which has a much weaker signal, extends southward towards the West Coast of Africa and further to the East Coast of Northern South America (Knight et al., 2005).

In addition to the AMV being the dominating mode of SST variability on a multidecadal timescale across the North Atlantic, it also has well known impacts on the climate and weather across the Northern Hemisphere. Examples of this include changes in North American and European climate (Enfield et al., 2001; Sutton and Hodson, 2005), Atlantic hurricane activity (Goldenberg et al., 2001; Knight et al., 2006), as well as affecting US, Sahel, and Amazonian rainfall (Enfield et al., 2001; Knight et al., 2006) to name a few. Despite the AMV being so influential to the climate, there is currently an ongoing scientific debate on the physics and core drivers behind it. Evidence of the AMV reaching as far back as the Holocene have been found by studying tree rings, corals, fossil pigments, and Greenland ice cores containing sea-spray (Knudsen et al., 2011). Despite this, the observational record of measurements only go back 150 years (Rayner et al., 2003), which is barely enough to cover two periods of the AMV. This makes drawing conclusions based on observations difficult. Instead, global climate models (GCM) can be used to investigate the AMV and its driving forces.

GCMs are a useful tool when modeling the Earth's intricate network of dynamical systems and their interactions. They take into account the underlying physics of fluid dynamics and thermodynamics that govern these systems. Some examples of fundamental physical principles underlining the physics in GCMs are the first law of thermodynamics (conservation of energy), Newton's 2nd law (conservation of momentum), and the continuity equation (conservation of mass). These equations ensure that the models obey the physical laws of nature and constitute the Navier-Stokes equations of fluid dynamics which govern the density, pressure, temperature, and speed of incompressible fluids (McSweeney, 2018). In a system like the atmosphere, air can be treated as incompressible as it is relatively slow
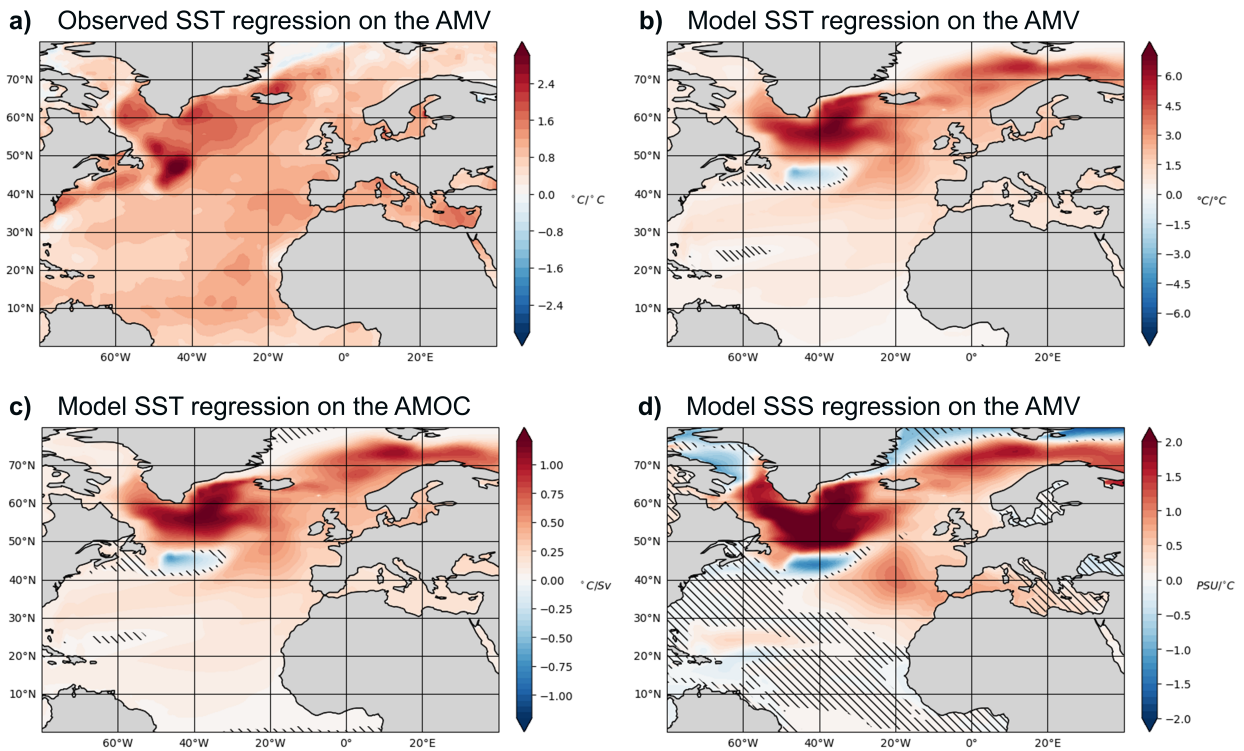
Figure 1: Regression maps of ocean surface variables against the AMV and AMOC indices in the North Atlantic. Positive (negative) values indicate an increase (decrease) in oceanic variable units per increase in index unit. 11-year running means have been applied to all the data. a) Observed SST ($°C$) from HadISST (Rayner et al., 2003) regressed on the observed AMV index. b) Model SST ($°C$) regressed on the AMV index. c) Model SST ($°C$) regressed on the AMOC index. d) Model SSS ($PSU = g/kg$) on the AMV index. Hatched bars indicate areas with non-statistically significant regions to the 99% level, as calculated according to Ebisuzaki (1997). Statistical test was not made for the observational data in a).

moving. However, these equations do not have an analytical solution and thus must be numerically solved in GCMs. Other important thermodynamic equations include the Stefan-Boltzmann's Law that regulates the radiation balance and the Clausius-Clapeyron equation, which relates temperature changes to changes in vapor pressure (McSweeney, 2018). Finally, a very important concept in meteorology is geostrophic balance. The geostrophic wind equation assumes that the Coriolis force, an apparent force caused by a rotating reference frame, is equally strong and acts opposite in direction to the pressure gradients in the atmosphere. This causes winds to move along lines of equal pressure (isobars) in the atmosphere. Thus, in a low pressure system in the Northern Hemisphere, winds rotate counterclockwise (cyclonic) and clockwise (anticyclonic) in a high pressure system.

The Coupled Model Intercomparison Project, which recently ended its sixth phase (CMIP6), is an international network with the goal of understanding the Earth's climate and how it is changing (Eyring et al., 2016). This is done mainly by comparing many different GCMs, as well as distributing model output data in a standardized format (Eyring et al., 2016; Meehl et al., 2000). Coupled general circulation models (CGCMs) are GCMs that take into account the interactions between different systems on Earth, like the atmosphere and oceans. Another type of GCM are Earth System Models (ESMs). They are more comprehensive than CGCMs as they do not only include the CGCM core of physical interactions between the atmosphere, ocean, sea ice, and land, but they also include various biophysical and biochemical processes (Döscher et al., 2022). One such ESM called EC-Earth3 was collaboratively developed by the European research consortium EC-Earth with the development goals of CMIP6 in mind, and it also serves to provide a useful tool for European universities and research institutes when studying the Earth's system (Döscher et al., 2022).

Some studies suggest that the Atlantic meridional overturning circulation (AMOC) is the main driver of the AMV (Knight et al., 2005; McCarthy et al., 2015; Zhang et al., 2019). The AMOC is a large network of ocean currents and is responsible for a significant northward heat transport across the equator into the North Atlantic (Meccia et al., 2022; Zhang et al., 2019). Warm, salty water in the upper layers of the Atlantic is transported northward, e.g. with the Gulf Stream, while deep cold water is transported southward. As with many dynamical systems in Earth's atmosphere and oceans, variability in the AMOC occurs naturally. Several other model studies have found that one of these modes of variability strongly correlate with the AMV (Brown et al., 2016; Drews & Greatbatch, 2016, 2017). Specifically, a positive correlation where it is believed that a stronger AMOC, that predates the AMV, increases the heat content in the North Atlantic on a multidecadal timescale resulting in the AMV.

While there are several frequency modes of variability in the AMOC with different drivers, one recent study using EC-Earth3 suggest that on longer timescales, sea ice and the salinity/density of the ocean modulates the AMOC (Meccia et al., 2022). Changes in salinity are intensified in the Arctic due to ice formation and melting and affects the AMOC variability on multidecadal to multicentennial timescales. Salty, more dense water lead to an increase in convection (downwelling) and the increased formation of deep water. Deep water formation is a key component of the AMOC (Meccia et al., 2022), and increased strength and variability in this formation lead to an increased strength and variability in the AMOC. Consequently, when the AMOC increases, more heat is transported northward, which in turn causes sea ice melting. When the sea ice melts there is a freshwater influx into the basin and the water column stabilizes which reduces the AMOC and the cycle repeats as the North Atlantic cools again. In the end, the link between the AMOC and AMV is not always consistent, as a recent study found that in a multi-model ensemble of pre-industrial CMIP6 simulations the AMV and AMOC experience multidecadal windows where they are

uncorrelated (Bellucci et al., 2022). These windows occurred when AMOC variability was lower than normal and could potentially leave room for other drivers of the AMV to take over.

Other drivers, that have been suggested by previous studies, are the atmospheric forcings of clouds (Clement et al., 2009) and aerosols (Booth et al., 2012), where some argue that atmospheric forcings are the main driver of the AMV (Clement et al., 2015), a fact that has been disputed by others (Drews & Greatbatch, 2016, 2017). Some suggest that atmospheric forcings are a necessary feedback to propagate SSTs into the subtropical region of the AMV (Bellomo et al., 2016; Brown et al., 2016; Yuan et al., 2016). However, the relationship between clouds and SSTs is a complex one, it varies between different regions and seasons in the North Atlantic. Clouds have two competing effects on the atmosphere's radiation budget: they reflect incoming solar radiation which cools the climate, but they also absorb longwave radiation emitted from the Earth and re-emit it in all directions, resulting in a warming of the climate. The effectiveness of these two different mechanisms differ depending on the height, thickness, and phase of the clouds and thus there is no simple answer to what effects clouds might have on SSTs in any given region. However, in the global mean, both clouds and aerosols serve to cool the climate as the reflectiveness on incoming solar radiation is thought to be generally higher than the warming effect (Randall et al., 2007). This is especially true for the low level clouds called stratocumulus. They have a very high cloud fraction which means that they scatter incoming solar radiation back more effectively than many other cloud types (Klein & Hartmann, 1993). They primarily occur over the eastern parts of ocean basins where SSTs are colder due to oceanic upwelling and a strong inversion layer is present in the low atmosphere. In the North Atlantic this low level inversion is called the Azores high and is necessary for the stratocumulus to form. It is thought to be maintained by sinking air (subsidence) in the descending part of the Hadley cell atmospheric circulation (Klein & Hartmann, 1993).

Studies looking at the pattern of SST variability in the AMV have found positive low-level cloud feedback with SSTs (Bellomo et al., 2016; Clement et al., 2009; Yuan et al., 2016; Zhou et al., 2017), where an increase in SSTs lead to a warming of the low atmosphere. This in turn decreases the air density which results in more rising air and a decrease in sea level pressure (SLP) over the North Atlantic. A lower pressure leads to a suppression in the Azores high pressure system, which in turn results in more cyclonic activity in the wind patterns. This disruption of the normal circulation pattern weakens the Northeasterly trade winds (Yuan et al., 2016) resulting in a less effective cooling of the ocean from wind advection. Reduced easterly winds also lead to less cold water upwelling on the eastern side of the North Atlantic basin as upwelling is controlled by zonal (East-West) wind induced advection. These two outcomes of lower wind speeds lead to further enhanced SSTs which causes the usually strong inversion in the subtropics to weaken, leading to less stratocumulus

formation (Brown et al., 2016; Klein & Hartmann, 1993; Yuan et al., 2016). The decreased cloud cover results in more incoming solar radiation to the surface of the ocean, increasing SSTs, thus closing the positive feedback loop between SST and cloud cover.

This thesis takes a first look at how EC-Earth3 models the AMV using a pre-industrial model run. In this run the atmospheric composition is fixed at the pre-industrial levels from the year 1870, thus ignoring external forcings such as the changes in aerosol content, volcanic emissions, as well as changes in greenhouse gasses that lead to climate change. This creates a more simple framework to study natural variability. The thesis compares the modeled AMV to the observed AMV, and investigates both the AMOC and total cloud cover as potential drivers for AMV with the aim of better understanding how the AMV behaves in EC-Earth3.

2 Model and Methods

2.1 A pre-industrial EC-Earth3 model run

A 1000-year-long pre-industrial ocean-atmosphere coupled model run of EC-Earth3 (piControl, ensemble member r5i1p1f1) was investigated in this thesis. The oceanic component of EC-Earth3 consists of the model: Nucleus for European Modelling of the Ocean (NEMO) version 3.6 (Gurvan et al., 2017) with the integrated sea-ice model Louvain la Neuve (Vancoppenolle et al., 2017). NEMO uses the tripolar grid, ORCA1L75, which has a horizontal resolution of $1°$ longitude by $1°$ latitude and 75 vertical levels. While the atmospheric component of EC-Earth3 consists of a modified cycle 36r4 Integrated Forecast System (ECMWF, 2004) using a T255L91 resolution which in turn corresponds to a horizontal resolution of about $80\,km$ and 91 vertical levels. Except for the AMOC, which is measured at $1000\,m$ depth, this analysis only considers the two-dimensional surface level dynamics.

2.2 The AMV and AMOC indices

The AMV index was created, as first proposed by Sutton and Hodson (2005) from anomalies in the area weighted yearly mean SSTs (measured in $°C$) in the area between $7.5 - 75°W$ and $0 - 60°N$ and then performing a 11-year running mean on these anomalies. This mean allows multidecadal trends to be more readily viewed as it averages from 5 years before to 5 years after each year in the time series. A secondary AMV index in the region $7.5 - 75°W$ and $0 - 45°N$ was calculated in order to study the subtropical arm of the AMV. Similarly, an AMOC index was also calculated by taking the anomalies of the yearly mean Atlantic meridional overturning streamfunction measured in Sverdrup ($1\,Sv = 10^6\,m^3$) at $1000\,m$ depth and

$45°N$, and then performing an 11-year running mean. The AMV and AMOC indices were compared by plotting their respective time series as well as calculating the correlation between them. In order to find at what temporal displacement the two indices best correlate, a cross correlation was calculated. This was done by shifting the AMOC index ahead or behind the AMV index in steps of one year at a time and then finding the maximum correlation. Finally, to check for any asymmetry between AMV warm and cold phases, composites of the AMV index were made by plotting SST anomalies, as well as total cloud cover anomalies, of the years experiencing index values of more than one standard deviation above (warm) or below (cold) the AMV index mean averaged over the entire time span.

2.3   Observational dataset

The observational dataset HadISST, retrieved from Met Office Hadley Centre (Rayner et al., 2003), records monthly SST values dating back to the year 1870 and up to present time. In order to remove the global warming trend and thus be able to compare the modeled AMV to the observed one, the observational AMV index was linearly de-trended by performing a least-squares fit. Power spectrum densities (PSDs) were calculated from the AMV indices from both observations and the model output using Welch's method, wherein a discrete Fourier Transform is applied to overlapping segmented parts of the respective time series. This approximates the discrete time series into many complex series in the frequency domain which are then averaged into PSDs that show the dominating frequencies found in the original time series. The period and power of the dominating frequency modes were then compared between the PSDs of the observed and modeled AMV indices. The PSDs of the subtropical AMV index was also calculated and compared to the regular AMV index in this analysis.

2.4   Post-processing of variables

In addition to the AMOC and SST output in the model run, other variables investigated in this thesis are sea surface salinity (SSS) given in practical salinity units ($PSU = g/kg$) as well as the atmospheric output variables of total cloud cover given in percentages, pressure at mean sea level (SLP) given in hPa, and a multitude of different surface heat fluxes given in Wm^{-2}. These aforementioned heat fluxes are the following: Shortwave downward heat flux representing the incoming solar radiation, shortwave upward heat flux representing the reflected solar radiation, longwave downward heat flux representing the warming effect of clouds and heating of the ocean, longwave upward heat flux representing the heat emitted by the ocean, latent heat flux representing the heat transport from evaporation and condensation occurring at the surface of the ocean, sensible heat flux representing the conductive heat transport at the surface of the ocean due to temperature differences.

Latent and sensible heat fluxes were investigated both separately and in combination by adding them together to represent the turbulent heat flux. Finally, all heat flux variables were combined into the net total heat flux. In this analysis only total cloud cover was available as a model output, but any anomalies in this variable on the multidecadal timescale as a result of SST changes is thought to mainly reflect the change in low-level clouds (Bellomo et al., 2016).

11-year running means of all atmospheric variables, as well as SST and SSS, were used as the dependent variables in regression analyses against the independent AMV index. An example of SST regressed against the AMV is seen in equation 1, where the variables with bars indicate the mean across the whole time span. These regressions are used as indicators of the linear relationships between the AMV and the dependent variables. By calculating the regression in each gridbox in the North Atlantic basin and then plotting it, the spatial pattern of changes in the measured variable during a high index AMV is revealed (Knight et al., 2005; Sutton & Hodson, 2005). A positive value means that as the AMV index increases by one unit, the dependent variable increases with the number of units represented by the strength of the regression. In the same way, observed SSTs were regressed against the observed AMV index, and the modeled SSTs were regressed against the AMOC index to show their linear relationships and spatial patterns. Additionally, the temporal evolution of all dependent variables were studied in lagged regression analyses, ranging from 50 years ahead of an AMV maximum to 50 years after an AMV maximum. This is done by shifting the dependent variable in time, both ahead of and behind the point of the AMV index maximum and then calculating the regression. Temporally shifted SSTs were also regressed against the AMOC index.

$$\sum_{years} \frac{(SST_{11yrrm} - \overline{SST}_{11yrrm})(AMV_{11yrrm} - \overline{AMV}_{11yrrm})}{(AMV_{11yrrm} - \overline{AMV}_{11yrrm})^2} \qquad (1)$$

All data used in this analysis are serially correlated, meaning that no year is independent from the previous years. This would normally lead to an underestimation of the true significance of the correlation between two time series, so in this thesis a method suggested by Ebisuzaki (1997) is used to calculate the statistical significance of the Pearson's correlation coefficients of serially correlated data. 500 random time series are first generated which all have the same PSDs as the original independent time series except the Fourier modes are randomly phase-shifted. A distribution made from the correlations between the random time series and the original dependent time series is then calculated. If the correlations between the two original time series fall outside of the 99th or 1st percentile of the random correlation distribution they are considered to be statistically significant.

3 Results and Discussion

3.1 How EC-Earth3 models the AMV

In the regression plot made with the observed HadISST data (Fig. 1a) changes in SSTs related to the AMV index are positive everywhere in the North Atlantic. This means that SSTs increase in the North Atlantic during a warm phase of the AMV, and decrease during a cold phase. However, a strong maximum in SST in the western subpolar Atlantic is visible around $45°N$ and $45°W$ and represents the subpolar arm of the AMV. When comparing the model (Fig. 1b) to observations (Fig. 1a), the subpolar arm of the AMV appears to have a relatively similar spatial distribution, other than a slight displacement to the Northeast in the model, which appears strongest at around $55°N$ and $35°W$. The signal in the model is also a lot stronger, having more than double the variation in SST to that of observations which can also be seen when comparing Fig. 2a and b. Another visible aspect of the observed SSTs in Fig. 1a are the relatively weak variations in SSTs along the western coast of Europe and Africa extending towards the East Coast of South America, which is the characteristic of the subtropical arm. However, in the model run, the anomalous SST signal in the subtropical arm is only marginally visible and does not extend as far south as in observations. A poorly modeled subtropical arm is a common problem that many climate models experience, where some models fail to reproduce the arm entirely (Yuan et al., 2016; Zhang et al., 2019).

The PSD (Fig. 3) of the observational data displays a mode of periods from around 60 years to above 100 years with a peak in signal at 74.5 years. This oscillatory behavior is also seen in the model data in Fig. 2b, where the most distinct oscillations occur between the years 2000-2600. Compared to observations, EC-Earth3 exhibits both a much higher amplitude and longer period, with a maximum at 128 years and high power signals extending above 200 years. This period is quite significantly longer than observations which is something also seen in other CMIP6 models (Bellucci et al., 2022), surpassing the multidecadal range and extending into the multicentennial range. For the purposes of this discussion, this thesis will continue to refer to this mode as the AMV.

While the long period is likely a discrepancy in the model, it is to be pointed out that the observational record is too short to definitively describe the true period of the AMV. Furthermore, early data is made up of ship based observations and often different methods of data collection are used in conjunction, which each have their own biases (Rayner et al., 2003). SST under sea ice is difficult to measure and in the observational data set values are missing early on. These missing data points show up as a temperature of $-1000°C$ in the data set, and had to be filtered out before a regression could be calculated.
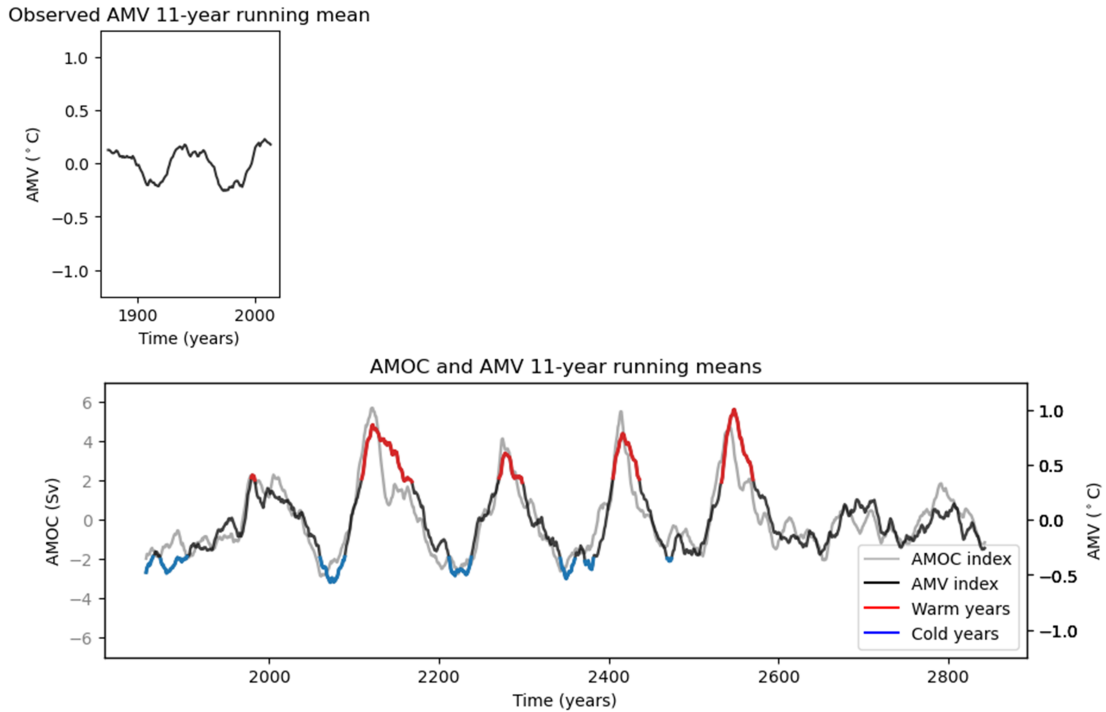
8

Figure 2: a) Calculated AMV index ($°C$) from observations (HadISST; Rayner et al., 2003) made from an 11-year running mean of linearly detrended SST anomalies in the region $7.5 - 75°W$ and $0 - 60°N$. b) model AMV (black) and AMOC (grey) index time series plotted together to display their similarities. The model AMV index is created from an 11-year running mean of SST anomalies in the region $7.5 - 75°W$ and $0 - 60°N$. Years that are one standard deviation warmer (colder) than the mean are plotted in red (blue). The AMOC index, measured in Sverdrup, is created from the 11-year running mean of the overturning circulation at $45°N$ and $1000\,m$ depth.

From the temporal analysis of the lagged regressions of SST on the AMV index (Fig. 4) it is clear that the maximum SST anomalies are found during the maximum AMV (0 lag) as per definition. Positive changes in SSTs start appearing 35 years before the AMV maximum (-35 lag) at the southern tip of Greenland and are not visible at all at 35 years behind the maximum (35 lag). This suggests that the AMV builds up SST anomalies over a longer time and once the maximum has passed the anomalies dissipate more rapidly. Another feature in the temporal evolution in Fig. 4 is a slight eastward shift in peak SST anomaly strength. Comparing the 20 year lag to the -20 year lag, the peak in SST anomalies appear more to the east of Greenland than where they started. This is a possible result of direct wind forcing as the mean wind direction propagates SSTs eastward over time.

Finally, the warm and cold composites were investigated in order to check for any asymmetry in the spatial distribution of the warm and cold phases of the AMV. Such
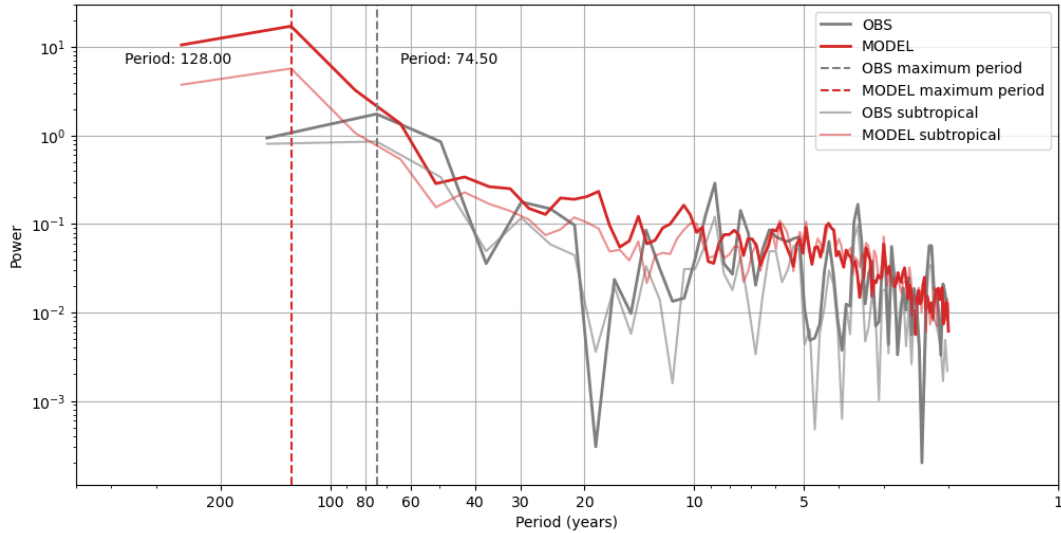
Figure 3: Power density spectrum (PSD) of the observed (grey) (HadISST; Rayner et al., 2003) and model (red) AMV index. Translucent PSDs are the subtropical AMV index. Higher power indicates a stronger signal in that period range, and high peaks in the multidecadal to multicentennial range are considered to be the AMV signal. The dotted lines indicate the period with highest power, 128 years for the model AMV and 74.5 years for observations.

an asymmetry was found in Baek et al. (2021) and was able to explain a change in subtropical SST, as cold SST anomalies were found to propagate into the subtropical region, while warm SST anomalies could not. Asymmetries in the composites are not found in this analysis as Fig. A.1a and b do not show any spatial asymmetry between years experiencing a warm or cold AMV phase. However, there is a slightly stronger signal during warm years. This can also be seen in Fig. 2b as warm years have a larger amplitude than cold years. Similar results were found in the total cloud cover composites in Fig. A.1c and d.

3.2 The relationship between the AMOC and AMV

When comparing the regression of SSTs on the AMV and AMOC indices the spatial distributions of changes in SSTs are essentially identical. There is a strong connection between the two indices (Fig. 2d) as the correlation calculated between them was found to be 0.893, a statistically significant result. The correlation even rises to 0.917 when the AMOC has a four year lead on the AMV, a result of the cross correlation analysis. The more delayed response of SSTs on the AMOC compared to the AMV is further reinforced in the lagged regressions. The first positive changes in SSTs in Fig. 5 appear closer to the AMOC maximum than they do the AMV max-
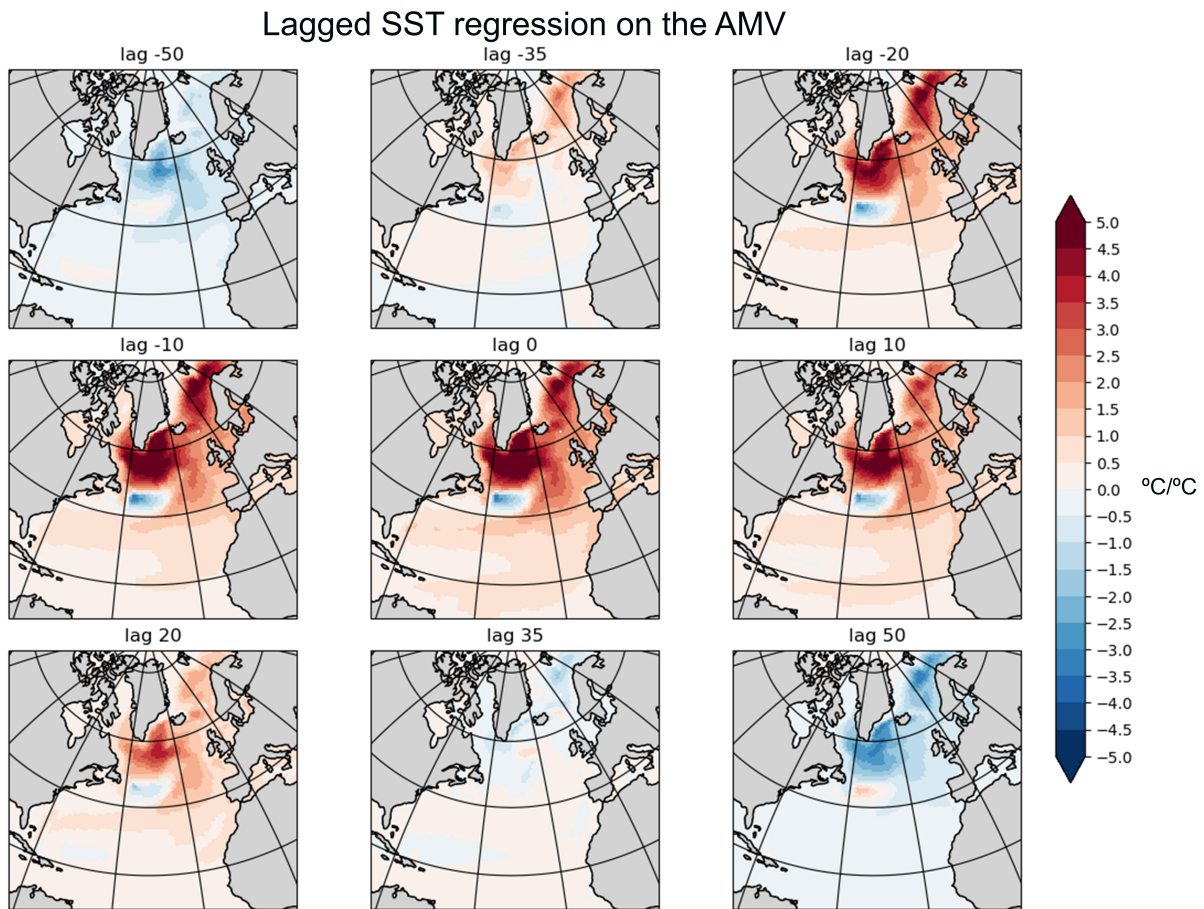
Figure 4: Regression maps of SST on the AMV index at different lag times in years where 11-year running means have been applied to the data. The colorbar indicates changes in °C in the North Atlantic per °C increase in the AMV index. Negative lag indicates number of years ahead of the AMV maximum.

imum in Fig. 4. Increases in SSTs are only first visible 20 years before the AMOC maximum in Fig. 5, and dissipate after 20 years. A very symmetrical temporal evolution compared to Fig. 4, which has more of an asymmetry around the maximum AMV. Similar lead times of the AMOC compared to the AMV are commonly found in both observations (McCarthy et al., 2015) and other models (Bellucci et al., 2022; Brown et al., 2016; Drews & Greatbatch, 2017), which is one of the key reasons the AMV is believed to be a delayed response in SSTs to the variability of the AMOC. Increased northward heat transport in the AMOC naturally leads to increased heat content in the North Atlantic and is thought to be the leading mechanism behind the initialization of the AMV (Zhang et al., 2019). Many CGCM hindcasts that take changes in external radiative forcing into account, are not able to predict the AMV if ocean initialization is not included (Zhang et al., 2019). However, after this initialization of the AMV other processes could be involved in propagating and amplifying
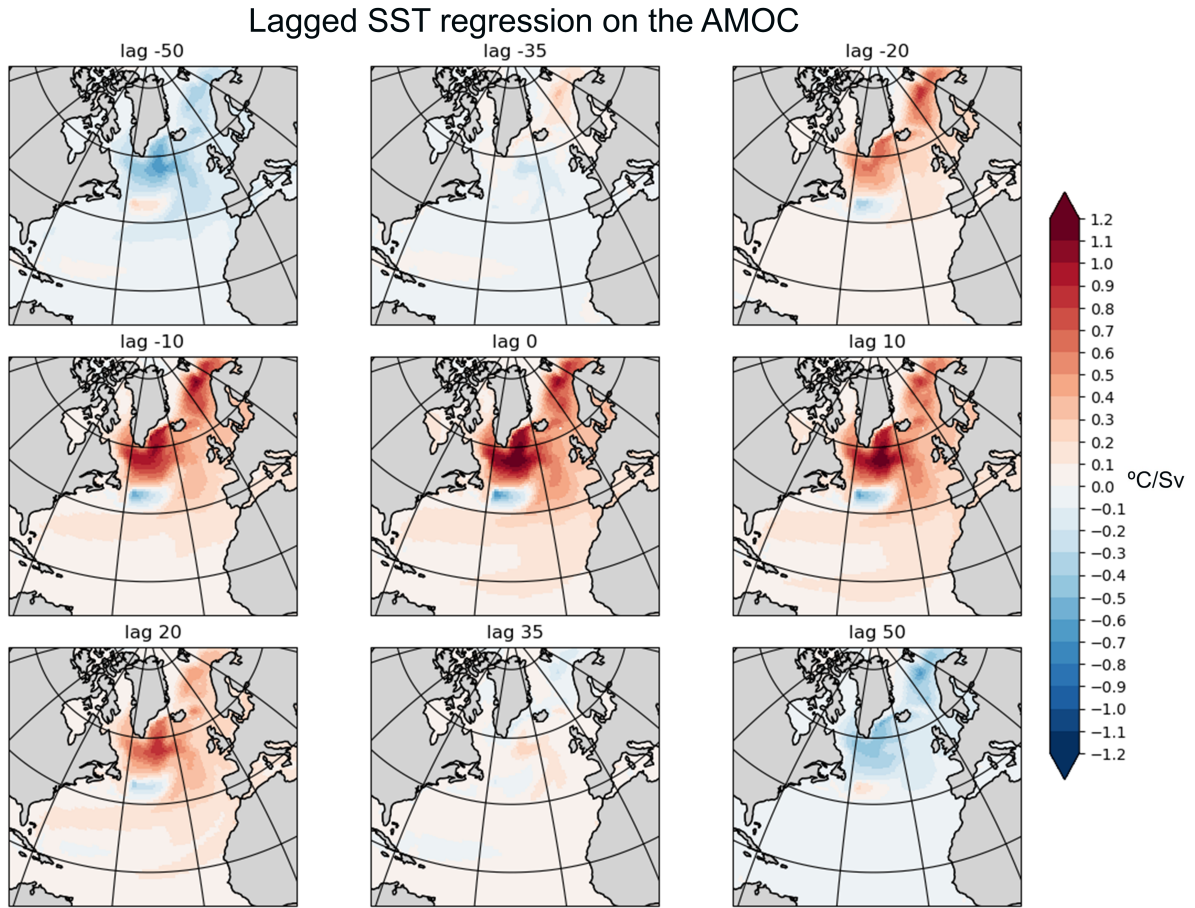
the SSTs of the AMV signal.

Figure 5: Regression maps of SST on the AMOC index at different lag times in years where 11-year running means have been applied to the data. The colorbar indicates changes in $^\circ C$ in the North Atlantic per Sv increase in the AMOC index. Negative lag indicates the number of years ahead of the AMOC maximum.

In EC-Earth3 the turbulent heat flux (Fig. 6d, positive upwards) is the dominating heat flux in the North Atlantic on multidecadal timescales. This is because the strength and spatial signal of the regressed turbulent heat flux versus the net total heat flux (Fig. 6c, positive upwards) are very similar. All other heat flux regressions (Fig. A.2, longwave not shown) have much lower regression values and thus contribute less to the net total heat flux. The spatial patterns in Fig. 6c and 6d, while more concentrated and not positive everywhere, are similar to that of the SST pattern associated with the AMOC and AMV. Previous model studies have found the same link between net upward heat flux and SSTs on multidecadal timescales (Drews & Greatbatch, 2016, 2017; Gulev et al., 2013; Zhang, 2017). It is believed that at low frequencies, a positive regression between net total surface heat flux and SST

anomalies indicate a stronger role for oceanic forcing as it is the ocean supplying the heat to the atmosphere, and not vice versa (Zhang 2017). This is another key reason why the AMOC is believed to modulate the AMV, which is supported by the results in this analysis as the net total heat flux in Fig. 6c overlaps well with the SST maximum in Fig. 1b. The positive heat flux indicates a heat loss into the atmosphere and would serve to dampen SST variations on the multidecadal timescale.
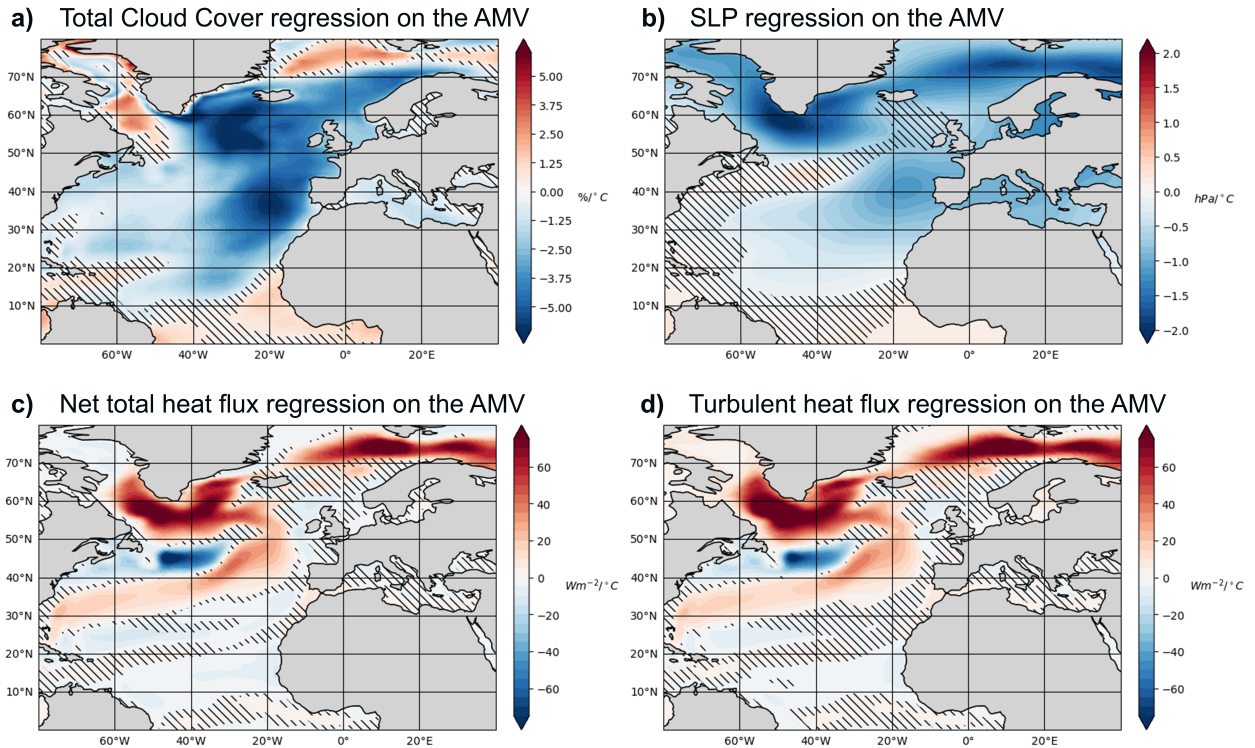

Figure 6: Regression maps of atmospheric variables against the AMV index in the North Atlantic. Positive (negative) values indicate an increase (decrease) in atmospheric variable units per increase in index unit. 11-year running means have been applied to all the data. a) Model total cloud cover in % regressed on the observed AMV index. b) Model SLP (hPa) regressed on the AMV index. c) Model net total heat flux (Wm^{-2}), positive upwards into the atmosphere, regressed on the AMV index. d) Model turbulent heat flux (Wm^{-2}), positive upwards into the atmosphere, on the AMV index. Hatched bars indicate areas with non-statistically significant correlations to the 99% level, as calculated according to Ebisuzaki (1997).

Furthermore, the analysis of SSS in Fig. 1d reinforce the result of an AMOC-driven modulation of the AMV. Salinity increases in the same region, and at the same time (Fig. 7) as SSTs do (Fig. 4), a result of the AMOCs northward transport of saltier and warmer water. However, this analysis does not investigate net precipitation (precipitation minus evaporation) which, if drastically changed, could affect salin-

ity. Sea ice melting is another influx of fresher water that is not investigated in this thesis. However, as sea ice melting occurs during a warm AMV SSS is decreased, working against the apparent increase in salt content during a warm AMV. This can be seen northeast of Greenland as negative regression values in fig. 1 and 7. On multidecadal timescales the ocean is thought to be the main driver of changes in SSS, and coherence between SST and SSS are only found at these long timescales (Zhang, 2017; Zhang et al., 2019). Thus from this analysis, variability in the AMOC seems to dominate SSS changes in the North Atlantic.
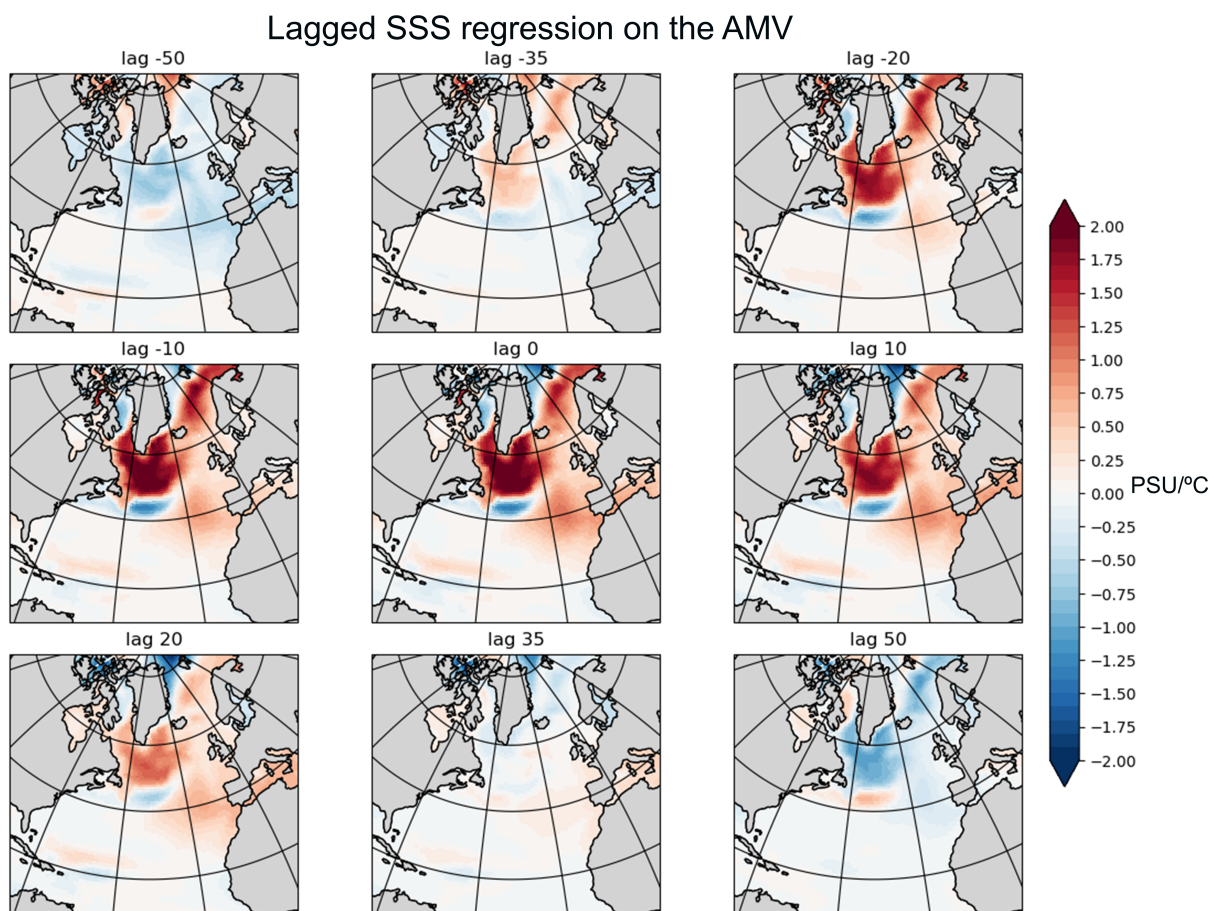

Figure 7: Regression maps of SSS on the AMV index at different lag times in years where 11-year running means have been applied to the data. The colorbar indicates changes in *PSU* in the North Atlantic per $°C$ increase in the AMV index. Negative lag indicates the number of years ahead of the AMV maximum.

The AMOC in EC-Earth3 is stronger and closer to observations than the CMIP5 ensemble mean of the previous EC-Earth model, version 2.3 (Döscher et al., 2022). If the AMV is indeed a delayed response to the AMOC, the increased amplitude of the AMOC could be amplifying the AMV. There are however likely other pro-

cesses contributing to the strong AMV in EC-Earth3. Additionally, the longer-than-observations period of the AMV could be explained by the long period of the AMOC in the model. This centennial to multicentennial mode of the AMOC is present in several other CMIP6 models (Bellucci et al., 2022). A possible explanation for the long AMOC period in EC-Earth3 could be that it has been found to model sea ice that extends too far into the Labrador, Greenland, and Barents seas (Döscher et al., 2022). Since AMOC variability is affected by sea ice melting and formation, due to the salinity and density variability it causes, this increase in sea ice fraction could explain why the AMOC has such a long period. Extended periods of sea ice melting could be keeping the AMOC in a weaker state for a longer period before it can recover and speed up again (Döscher et al., 2022; Meccia et al., 2022).

It is also worth noting that the significant SST regression signals south of the Labrador sea, Greenland sea, extending towards Barents sea, in Fig. 1b and c is likely due to the southward displaced sea ice in EC-Earth3 that is experiencing melting during warm AMV years. This signal is also present in most other regression maps in this analysis and reflects how sea ice melts and significantly changes the temperature and behavior of those areas. Specifically, the upwards shortwave heat flux (Fig. A.2a) show a strong negative regression in the regions believed to be experiencing melting sea ice. As the ice melts, the albedo of the surface of the North Atlantic in those regions is drastically reduced, causing less solar radiation to be reflected back, thus amplifying the SST variability there.

A region of negative regressions is present in all the modeled oceanic variables (Fig. 1b, c and d) and is found at $45°N$ and $40°W$. This negative anomaly is also found in the heat flux maps Fig. 6c and d, and is likely EC-Earth3s representation of the dipole pattern caused by the AMOC in observations, called the AMOC fingerprint (Zhang et al., 2019). On a multidecadal timescale, stronger AMOC is triggered by increased deep water formation. This has been found to be coupled with a southward shift in the Gulf Stream, which occurs due to changes in the different North Atlantic oceanic horizontal gyres (Zhang et al., 2019). When this shift occurs, SSTs become anomalously colder in this region that would normally transport warm Gulf Stream water. The turbulent and net total heat fluxes (Fig. 6c and d) show this pattern even better, as a positive regression is shown South of the AMOC fingerprint. This is likely where the Gulf Stream has been shifted to, and is why this region experiences an increased heat loss to the atmosphere due to an increased warm water transport.

So far, the AMOC has been suggested to play a role in the formation of the subpolar arm while likely affecting subtropical regions less. Investigating the subtropical part of the AMV in Fig. 3 and A.3 it is clear that it does not vary from the whole AMV in any significant way other than an expected reduction in amplitude. This appears as a stronger SST variation in Fig. A.3 due to the lower amplitude AMV index. Thus, the subtropical arm does not operate on any additional mode of frequencies from

the rest of the AMV. It does however appear around sometime around 15 years later than the subpolar arm of the AMV as seen in lag -35 and -20 in Fig. 4. This suggests that the AMV is initialized in the subpolar region and then propagates southward over time. Changes in SSS in Fig. 7 also appear in the subtropical region later. Since this variability is mainly forced by the ocean it could potentially point to some level of AMOC activity in this region, but it is considerably lower than in the subpolar region. Oceanic upwelling could be playing a role in the SSS changes in this region, but it is not investigated in this thesis as only surface dynamics and the AMOC stream function are considered. Therefore, this analysis concludes that the AMOC likely initializes and modulates the AMV in EC-Earth3 but leaves room for other feedbacks to help propagate SST anomalies southward.

3.3   Atmosphere dynamics and responses

Total cloud cover (Fig. 6a) has a clear negative response slightly downwind of the SST anomalies associated with the AMV (Fig. 1b). Thus, when the AMV is in a warm (cold) phase the North Atlantic experiences anomalously low (high) cloud cover. Changes in total cloud cover occurring downwind of initial SST anomalies suggests that the cloud cover does not initialize the SST anomalies. However, they are still likely amplifying changes in SSTs downwind of the initial anomaly as a reduction (increase) in cloud cover leads to an increase (reduction) in incoming solar radiation. The temporal analysis of the total cloud cover in Fig. 8 shows that total cloud cover anomalies do not occur before the SST anomalies in Fig. 4 but instead have a very similar temporal evolution. Since the atmosphere has a quicker response time than the ocean (Yuan et al., 2016), this supports the theory that cloud cover is not the origin of SST change but rather a response to the initial changes in SSTs caused by some other factor, like the AMOC.

The anomalously low SLP in the North Atlantic (Fig. 6b) suggest that there is more cyclonic wind activity during a warm AMV phase. This does not mean however, that there is a cyclonic wind pattern during a high index AMV, but instead that the winds tend to be either more cyclonic or less anti-cyclonic during warm years, and vice versa for cold years. Negative SLP anomalies already appear in relative strength around the southern tip of Greenland 35 years before the AMV maximum (Fig. 9) and experiences a peak in strength at the 10 years lead time. This is a rather significant asymmetry around the AMV maximum as SLP anomalies are not visible at all at 35 years lag. While SST anomalies also start to show up around this time (Fig. 4), it is interesting that the maximum SLP signal South of Greenland is ahead of the AMV maximum. The maximum SLP for the subtropical region however occurs at lag 0. This points to the fact that the atmospheric response to initial SST anomalies amplifies the SST anomalies so that the maximum occurs later and that there is a slight delayed response in the subtropics compared to the subpolar region.
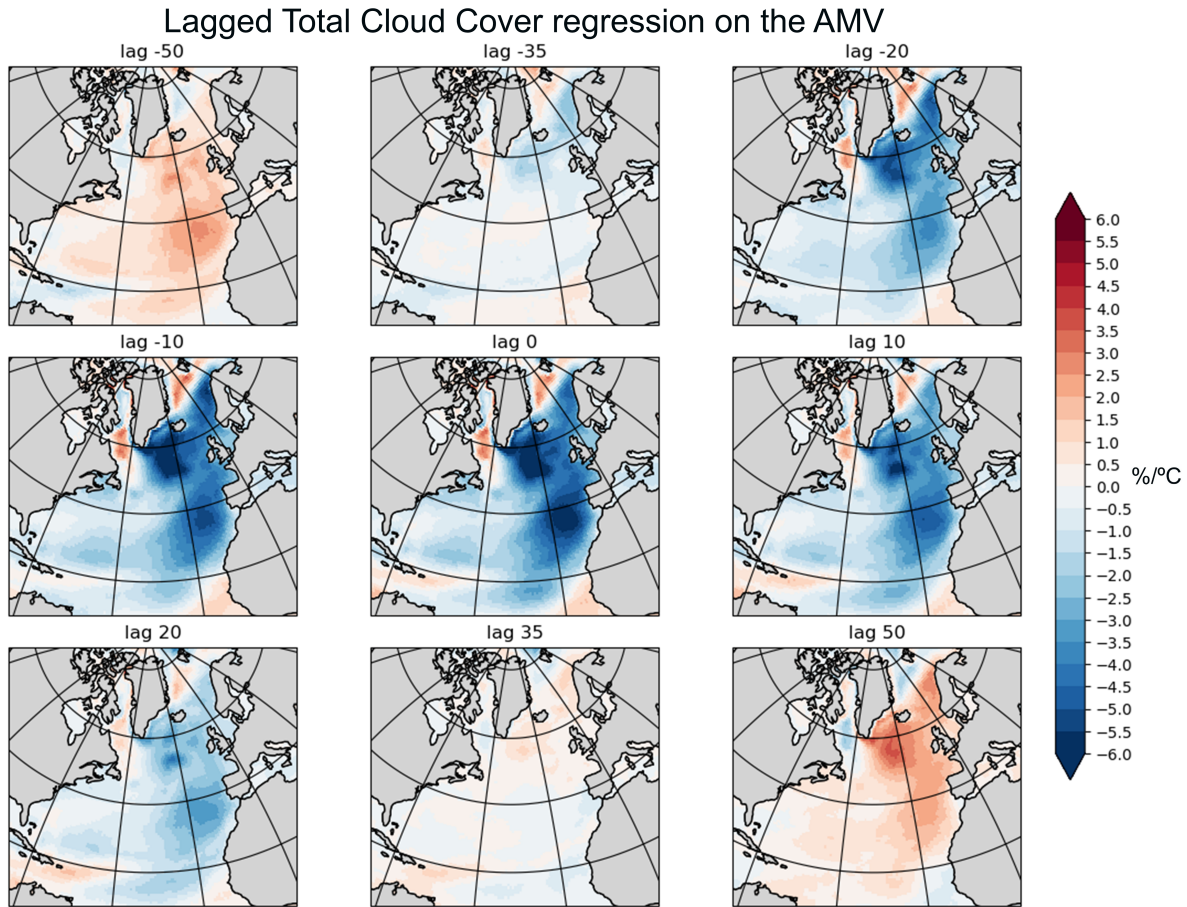
Figure 8: Regression maps of total cloud cover on the AMV index at different lag times in years where 11-year running means have been applied to the data. The colorbar indicates changes in % total cloud cover change in the North Atlantic per $°C$ increase in the AMV index. Negative lag indicates the number of years ahead of the AMV maximum.

The strongest signal of reduced SLP South of Greenland is likely caused by the steep increase in SSTs as sea ice melts in the early positive phase of the AMV. In this region a subpolar low pressure system, called the Icelandic low, is already a prominent feature, and the lower pressure during a warm AMV would serve to deepen this low. Yuan et al. (2016) explain that in observations the decreased SLP center is located in the middle of the North Atlantic and the southwesterlies in the southern part of this anomalous low pressure weaken the northeasterly trade winds which reduces wind speeds in the subtropical region. It is possible that this negative signal in EC-Earth3 is displaced northward due to a stronger effect of sea ice melting South of Greenland. But this would need to be verified in an analysis of the sea ice fraction and water density changes.
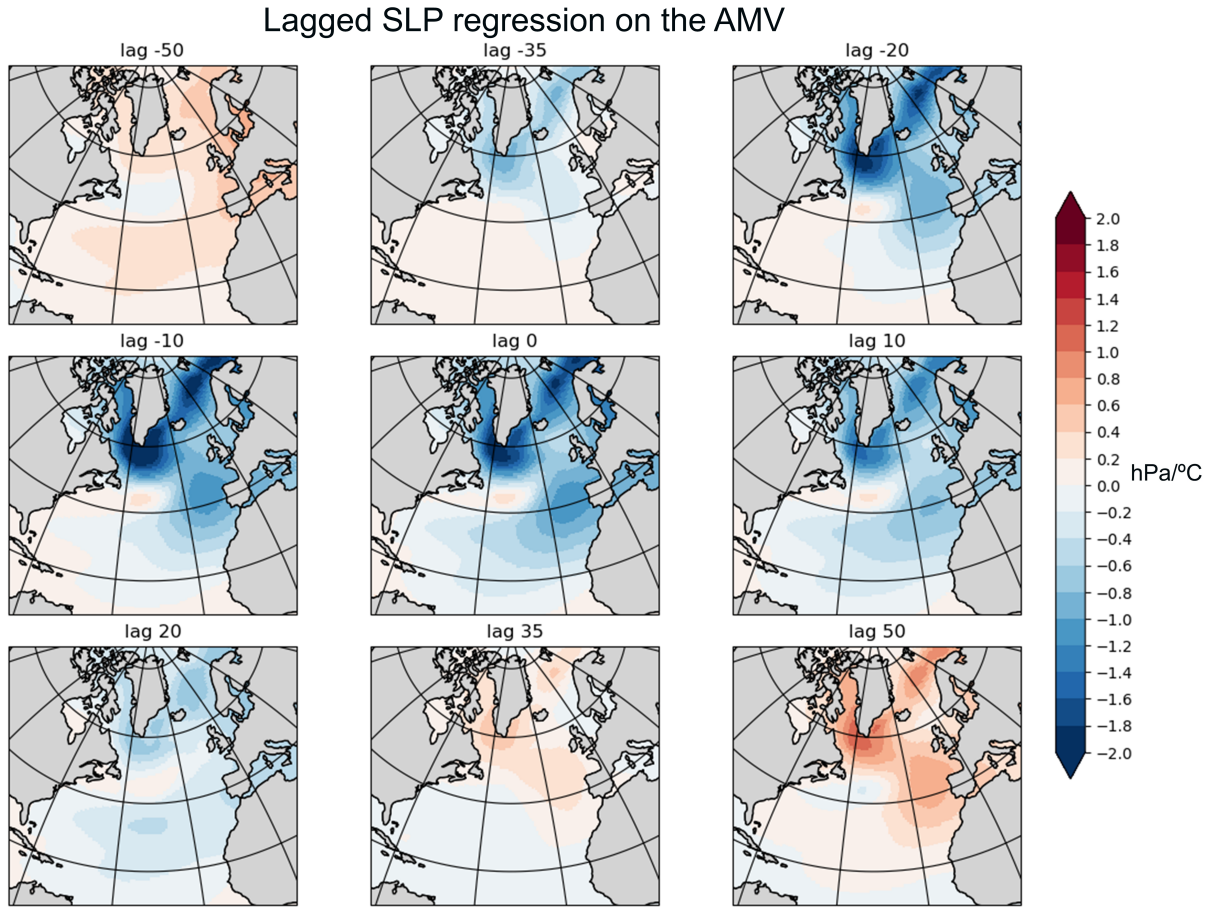
Figure 9: Regression maps of SLP on the AMV index at different lag times in years where 11-year running means have been applied to the data. The colorbar indicates changes in *hPa* in the North Atlantic per °*C* increase in the AMV index. Negative lag indicates the number of years ahead of the AMV maximum.

Furthermore, the negative regression signal in SLP around $40°N$ and $20°W$ (Fig. 6b), that occurs later than the subpolar low, serves to weaken the Azores high pressure system, which in turn weakens the trade winds. This center of lower SLP forms due to increased SSTs in this region, and could be initialized by a multitude of factors, likely a combination of increased AMOC, as well as reduced northeasterly trade winds causing reduced oceanic cooling and upwelling. Changes in horizontal circulation gyres could potentially also play a role but further analysis would be necessary to confirm why this anomaly occurs as a delayed reaction to the AMV in EC-Earth3. Nevertheless, the suppression in the Azores high is a common feature found during a positive AMV phase (Bellomo et al., 2016). Reduced subsidence in this region results in stratocumulus clouds becoming less likely to form, which causes a positive feedback between cloud cover and SSTs and is seen as a strong negative regression in the subtropical region in Fig. 6a where cloud cover is reduced on

a multidecadal timescale in connection to the AMV. Changes of opposite sign occur during the cold AMV phase as seen in Fig. A.1d (Bellomo et al., 2016). As winds generally blow towards the east in the subtropical and tropical region, this leaves a potential for the cloud signals to be advected across the North Atlantic and spread the changes in SSTs to these regions associated with the subtropical arm of the AMV in observations. However, EC-Earth3 poorly replicates this process as cloud cover and SST have poor regression signals across the subtropical North Atlantic.

The warming effect of the atmosphere on the ocean is visible in the very small negative net total heat flux along the West Coast of Europe and in southern parts of the North Atlantic in Fig. 6c. This is potentially due to cloud feedback, as incoming solar radiation is stronger in the subtropics/tropics causing it to have a higher sensitivity to changes in cloud cover. These regions of ocean heating are less visible in the turbulent heat flux 6d, and instead likely come from the downwards shortwave heat flux (Fig. A.2b). Making note of the smaller colorbar ranges compared to Fig.6c and d, positive regressions can be seen in the same regions as the negative regressions of total cloud cover (Fig. 6a). This indicates that as cloud cover is reduced in this region, the atmosphere heats the ocean through increased incoming solar radiation. In the end, this analysis suggests that positive cloud feedback is present in EC-Earth3 and helps propagate the AMV subtropical arm southward. Since the subtropical arm is not as strong in the model as it is in observations, it could mean that the cloud feedback is not strong enough, or that other feedbacks are missing from the model.

3.4 Study and model and limitations

This thesis only investigated one pi-control run on one model, and an important factor of model assessment is looking at several different types of model runs. Such a study should include historical runs which mimic the atmospheric composition measured in observations (McSweeney, 2018). Historical runs may mimic reality more closely as long-term changes in atmospheric composition occur. Perhaps such trends could even be necessary for a more accurate AMV. However, there is also a risk that these trends can dominate natural variability making models not able to reproduce the AMV at all. This is why it is important to run both historical simulations as well as pre-industrial control runs. Furthermore, multiple historical runs of EC-Earth3 with different initial states could be compared. This comparison would help to distinguish between external forcing signals and the internal variability within EC-Earth3. Multiple model runs studied collectively, called an ensemble, allow for the calculation of an ensemble mean. Ensemble means better represents the central tendency of the model, reducing the impact of random variability or noise present in any single model run. Finally, so-called "ocean-only" models can separate variability driven by atmospheric forcings from oceanic ones (McSweeney, 2018). A

ocean-only configuration in EC-Earth3 could be another topic of investigation since the atmospheric influence on the AMV is under debate. It is likely that EC-Earth3 would still be able to produce an AMV signal, but it would be interesting to see how the period, amplitude, and spatial signal changes.

CMIP6 consists of many other models (Eyring et al., 2016) and if the dynamics of the AMV are to be better understood, ensembles of many different models can offer great insight into the AMV, as models might have different underlying mechanics that modulate it. This is why projects such as CMIP6 are important. It allows common trends in models to be found, increasing confidence in them being based in reality. Running many models with the same boundary conditions would highlight differences and potential discrepancies between the models. This type of study would be beneficial for evaluating EC-Earth3 and would allow one to draw more robust conclusions about the AMV.

Other model variables, not investigated in this thesis, could offer a greater insight to the AMV-AMOC relationship. One phenomenon in need of assessment is the deep convection in the ocean as it is a huge part of the AMOC (Meccia et al., 2022; Zhang, 2017). Sea ice formation and melting changes the density of water and thus affects the rate of deep convection in the ocean. If this is affecting the AMOC it would be affecting the AMV as well through their apparent connection. Therefore, sea ice fraction would be a promising variable to assess in EC-Earth3, especially since many variables have large regression values in the regions that are believed to be experiencing a change in sea ice fraction. Checking if precipitation is severely changed in these regions would help verify if it is indeed the sea ice fraction dominating the density changes of the surface of the ocean. Finally, dynamics of the North Atlantic oscillation (NAO) and North Atlantic subpolar gyre are also crucial elements that need to be evaluated in relation to the AMOC and AMV, as they could be affecting the large scale circulation in the basin through their own variability and oscillations (Sutton et al., 2018; Zhang et al., 2019). These aforementioned variables and processes could potentially highlight why the model AMV experiences such a strong, low-frequency variability compared to the AMV in observations.

Atmospheric feedbacks could also be further understood by investigating the aforementioned variables and processes, especially if done in the subtropical region. Salinity and upwelling could help confirm why initial changes in subtropical SSTs occur. By studying atmospheric and oceanic circulation, like the NAO and oceanic gyres, the propagation of SST anomalies southward could also be better understood, both in regards to cloud feedback but also through direct wind and gyre forcing. Furthermore, as this analysis investigates a pre-industrial run, aerosol loading in the atmosphere remains unchanged. Aerosols are an important factor for cloud formation and changes in aerosol loading could be a missing positive feedback necessary for the subtropical arm to fully form (Yuan et al., 2016). Thus, as previously stated,

historical simulations that account for aerosols are an important next step in understanding the role that positive cloud feedback plays in the AMV.

Finally, all regression maps made in this analysis, except for the observed SSTs, were put through a statistical significance test to reject the null hypothesis of the correlation being random noise. The tests were performed at the 99% confidence interval, which is a high bar. This analysis finds that all of the regression maps are statistically significant almost everywhere in the North Atlantic. Only marginal regions, usually not of interest to this analysis, lack statistical significance. Thus it is concluded that the signals are overall statistically significant in the regions of interest.

4   Conclusions and Outlook

This analysis was focused on how EC-Earth3 models the AMV and investigated potential underlying connections to different model variables. The natural variability of SST in the North Atlantic was investigated in a pre-industrial run of 1000 years and a variability was found in the centennial timescale with a period of around 128 years. This signal is considered to be the model AMV, despite the longer period and higher amplitude than in observations. Further assessment is needed in order to understand why this discrepancy occurs, but one theory is the high contents of sea ice in the Labrador sea causing the AMOC to have a longer period. The correlation between the AMOC and AMV is found to be very high, strongest when the AMOC has a four year lead on the AMV. While this analysis suggests that the AMV is a result of AMOC variability, it is likely not as simple a solution to say that the AMOC causes the AMV, but rather that it plays some role in its creation and modulation. If the AMV and AMOC experience uncoupled periods of time, the mechanics of this uncoupling would need to be better understood in order for climate models to better simulate the AMV and increase their prediction skills.

Furthermore, this analysis finds that cloud feedback is likely amplifying the AMV and causing the maximum AMV to occur later, while also propagating changes in SSTs southward causing a small subtropical arm to appear in the model. The main mechanic behind this suggested in the thesis is that a reduction in SLP caused by a warming North Atlantic, causes the northeasterly trade winds over the subtropics to decrease. This leads to reduced oceanic cooling and upwelling, which in turn further enhances SSTs in this region, lowering the pressure in the subtropics. This lowered pressure reduces subsidence and thus reduces the amount of stratocumulus which results in a positive feedback between SSTs and cloud cover. Since this subtropical arm is less prominent than in observations there is likely some missing feedbacks necessary in order to fully form the subtropical arm. One suggested feedback mechanism is aerosols, as they enhance cloud formation and alter the Earth's radiation budget due to direct scattering and re-emission of longwave radiation.

As highlighted in section 3.4, the next step for a deeper analysis of the AMV in EC-Earth3 would be to include more model variables, such as sea ice fraction, water density, precipitation, and horizontal as well as deep oceanic/atmospheric circulation. Additionally, investigating one or more historical runs of EC-Earth3 would be a useful way to determine if aerosols, which hold a potential for increased cloud feedback, and other external forcings play a role in the AMV.

In the end, the effects of the observed AMV are felt throughout the Northern Hemisphere, and a better understanding of its underlying mechanisms is crucial for GCMs and their prediction skills. EC-Earth3 is able to reproduce the AMV in a pre-industrial control run, however, whether it is a very realistic AMV is questionable. Further analysis of the AMV, both in EC-Earth3, and other CMIP6 models are vital for future research as the climate is changing. These changes could have unforeseen impacts on the AMV and thus risk substantially changing the weather and climate in the Northern Hemisphere.

Acknowledgements

References

Baek, S. H., Kushnir, Y., Robinson, W. A., Lora, J. M., Lee, D. E., & Ting, M. (2021). An Atmospheric Bridge Between the Subpolar and Tropical Atlantic Regions: A Perplexing Asymmetric Teleconnection. *Geophysical Research Letters*, *48*(24), e2021GL096602. https://doi.org/10.1029/2021GL096602

Bellomo, K., Clement, A. C., Murphy, L. N., Polvani, L. M., & Cane, M. A. (2016). New observational evidence for a positive cloud feedback that amplifies the Atlantic Multidecadal Oscillation. *Geophysical Research Letters*, *43*(18), 9852–9859. https://doi.org/10.1002/2016GL069961

Bellucci, A., Mattei, D., Ruggieri, P., & Famooss Paolini, L. (2022). Intermittent Behavior in the AMOC-AMV Relationship. *Geophysical Research Letters*, *49*(17), e2022GL098771. https://doi.org/10.1029/2022GL098771

Booth, B., B. B., Dunstone, N. J., Halloran, P. R., Andrews, T., & Bellouin, N. (2012). Aerosols implicated as a prime driver of twentieth-century North Atlantic climate variability. *Nature*, *484*(7393), 228–232. https://doi.org/10.1038/nature10946

Brown, P. T., Lozier, M. S., Zhang, R., & Li, W. (2016). The necessity of cloud feedback for a basin-scale Atlantic Multidecadal Oscillation. *Geophysical Research Letters*, *43*(8), 3955–3963. https://doi.org/10.1002/2016GL068303

Clement, Amy, Bellomo, K., Murphy, L. N., Cane, M. A., Mauritsen, T., Rädel, G., & Stevens, B. (2015). The Atlantic Multidecadal Oscillation without a role for ocean circulation. *Science*, *350*(6258), 320–324. https://doi.org/10.1126/science.aab3980

Clement, C., A., Burgman, R., & Norris, J. R. (2009). Observational and Model Evidence for Positive Low-Level Cloud Feedback. *Science*, *325*(5939), 460–464. https://doi.org/10.1126/science.1171255

Döscher, R., Acosta, M., Alessandri, A., Anthoni, P., Arsouze, T., Bergman, T., Bernardello, R., Boussetta, S., Caron, L.-P., Carver, G., Castrillo, M., Catalano, F., Cvijanovic, I., Davini, P., Dekker, E., Doblas-Reyes, F. J., Docquier, D., Echevarria, P., Fladrich, U., . . . Zhang, Q. (2022). The EC-Earth3 Earth system model for the Coupled Model Intercomparison Project 6. *Geoscientific Model Development*, *15*(7), 2973–3020. https://doi.org/10.5194/gmd-15-2973-2022

Drews, A., & Greatbatch, R. J. (2016). Atlantic Multidecadal Variability in a model with an improved North Atlantic Current. *Geophysical Research Letters*, *43*(15), 8199–8206. https://doi.org/10.1002/2016GL069815

Drews, A., & Greatbatch, R. J. (2017). Evolution of the Atlantic Multidecadal Variability in a Model with an Improved North Atlantic Current. *Journal of Climate*, *30*(14), 5491–5512. https://doi.org/10.1175/JCLI-D-16-0790.1

Ebisuzaki, W. (1997). A Method to Estimate the Statistical Significance of a Correlation When the Data Are Serially Correlated. *Journal of Climate*, *10*(9), 2147–2153. https://doi.org/10.1175/1520-0442(1997)010<2147:AMTETS>2.0.CO;2

ECMWF. (2004). IFS Documentation CY36R1 - Part IV: Physical Processes. Retrieved May 5, 2023, from https://www.ecmwf.int/en/elibrary/74350-ifs-documentation-cy36r1-part-iv-physical-processes

Enfield, D. B., Mestas-Nuñez, A. M., & Trimble, P. J. (2001). The Atlantic Multidecadal Oscillation and its relation to rainfall and river flows in the continental U.S. *Geophysical Research Letters*, *28*(10), 2077–2080. https://doi.org/10.1029/2000GL012745

Eyring, V., Bony, S., Meehl, G. A., Senior, C. A., Stevens, B., Stouffer, R. J., & Taylor, K. E. (2016). Overview of the Coupled Model Intercomparison Project Phase 6 (CMIP6) experimental design and organization. *Geoscientific Model Development*, *9*(5), 1937–1958. https://doi.org/10.5194/gmd-9-1937-2016

Goldenberg, S. B., Landsea, C. W., Mestas-Nuñez, A. M., & Gray, W. M. (2001). The Recent Increase in Atlantic Hurricane Activity: Causes and Implications. *Science*, *293*(5529), 474–479. https://doi.org/10.1126/science.1060040

Gulev, S. K., Latif, M., Keenlyside, N., Park, W., & Koltermann, K. P. (2013). North Atlantic Ocean control on surface heat flux on multidecadal timescales. *Nature*, *499*(7459), 464–467. https://doi.org/10.1038/nature12268

Gurvan, M., Bourdallé-Badie, R., Bouttier, P.-A., Bricaud, C., Bruciaferri, D., Calvert, D., Chanut, J., Clementi, E., Coward, A., Delrosso, D., Ethé, C., Flavoni, S., Graham, T., Harle, J., Iovino, D., Lea, D., Lévy, C., Lovato, T., Martin, N., . . . Vancoppenolle, M. (2017). NEMO ocean engine. https://doi.org/10.5281/ZENODO.3248739

Klein, S. A., & Hartmann, D. L. (1993). The Seasonal Cycle of Low Stratiform Clouds. *Journal of Climate*, *6*(8), 1587–1606. https://doi.org/10.1175/1520-0442(1993)006<1587:TSCOLS>2.0.CO;2

Knight, J. R., Allan, R. J., Folland, C. K., Vellinga, M., & Mann, M. E. (2005). A signature of persistent natural thermohaline circulation cycles in observed climate. *Geophysical Research Letters*, *32*(20). https://doi.org/10.1029/2005GL024233

Knight, J. R., Folland, C. K., & Scaife, A. A. (2006). Climate impacts of the Atlantic Multidecadal Oscillation. *Geophysical Research Letters*, *33*(17). https://doi.org/10.1029/2006GL026242

Knudsen, M. F., Seidenkrantz, M.-S., Jacobsen, B. H., & Kuijpers, A. (2011). Tracking the Atlantic Multidecadal Oscillation through the last 8,000 years. *Nature Communications*, *2*(1), 178. https://doi.org/10.1038/ncomms1186

McCarthy, G. D., Haigh, I. D., Hirschi, J. J.-M., Grist, J. P., & Smeed, D. A. (2015). Ocean impact on decadal Atlantic climate variability revealed by sea-level observations. *Nature*, *521*(7553), 508–510. https://doi.org/10.1038/nature14491

McSweeney, R. (2018). Q&A: How do climate models work? Retrieved April 26, 2023, from https://www.carbonbrief.org/qa-how-do-climate-models-work/

Meccia, V. L., Fuentes-Franco, R., Davini, P., Bellomo, K., Fabiano, F., Yang, S., & von Hardenberg, J. (2022). Internal multi-centennial variability of the Atlantic

Meridional Overturning Circulation simulated by EC-Earth3. *Climate Dynamics*. https://doi.org/10.1007/s00382-022-06534-4

Meehl, G. A., Boer, G. J., Covey, C., Latif, M., & Stouffer, R. J. (2000). The Coupled Model Intercomparison Project (CMIP). *Bulletin of the American Meteorological Society*, *81*(2), 313–318. Retrieved April 6, 2023, from https://www.jstor.org/stable/26215108

Randall, D. A., Wood, R. A., Bony, S., Colman, R., Fichefet, T., Fyfe, J., Kattsov, V., Pitman, A., Shukla, J., Srinivasan, J., Stouffer, R. J., Sumi, A., Taylor, K. E., AchutaRao, K., Allan, R., Berger, A., Blatter, H., Bonfils, C., Boone, A., . . . McAvaney, B. (2007). Climate Models and Their Evaluation.

Rayner, N. A., Parker, D. E., Horton, E. B., Folland, C. K., Alexander, L. V., Rowell, D. P., Kent, E. C., & Kaplan, A. (2003). Global analyses of sea surface temperature, sea ice, and night marine air temperature since the late nineteenth century. *Journal of Geophysical Research*, *108*(D14), 4407. https://doi.org/10.1029/2002JD002670

Schlesinger, M., & Ramankutty, N. (1994). An Oscillation in the global climate system of period 65–70 years. *Nature*, *367*, 723–726. https://doi.org/10.1038/367723a0

Sutton, R. T., McCarthy, G. D., Robson, J., Sinha, B., Archibald, A. T., & Gray, L. J. (2018). Atlantic Multidecadal Variability and the U.K. ACSIS Program. *Bulletin of the American Meteorological Society*, *99*(2), 415–425. https://doi.org/10.1175/BAMS-D-16-0266.1

Sutton, R. T., & Hodson, D. L. R. (2005). Atlantic Ocean forcing of North American and European summer climate. *Science (New York, N.Y.)*, *309*(5731), 115–118. https://doi.org/10.1126/science.1109496

Vancoppenolle, Martin, & Tedesco, L. (2017). Numerical models of sea ice biogeochemistry. In *Sea Ice: Third Edition* (pp. 492–515). https://doi.org/10.1002/9781118778371.ch20

Yuan, T., Oreopoulos, L., Zelinka, M., Yu, H., Norris, J. R., Chin, M., Platnick, S., & Meyer, K. (2016). Positive low cloud and dust feedbacks amplify tropical North Atlantic Multidecadal Oscillation. *Geophysical Research Letters*, *43*(3), 1349–1356. https://doi.org/10.1002/2016GL067679

Zhang, R. (2017). On the persistence and coherence of subpolar sea surface temperature and salinity anomalies associated with the Atlantic multidecadal variability. *Geophysical Research Letters*, *44*(15), 7865–7875. https://doi.org/10.1002/2017GL074342

Zhang, R., Sutton, R., Danabasoglu, G., Kwon, Y.-O., Marsh, R., Yeager, S. G., Amrhein, D. E., & Little, C. M. (2019). A Review of the Role of the Atlantic Meridional Overturning Circulation in Atlantic Multidecadal Variability and Associated Climate Impacts. *Reviews of Geophysics*, *57*(2), 316–375. https://doi.org/10.1029/2019RG000644

Zhou, C., Zelinka, M. D., & Klein, S. A. (2017). Analyzing the dependence of global cloud feedback on the spatial pattern of sea surface temperature change with
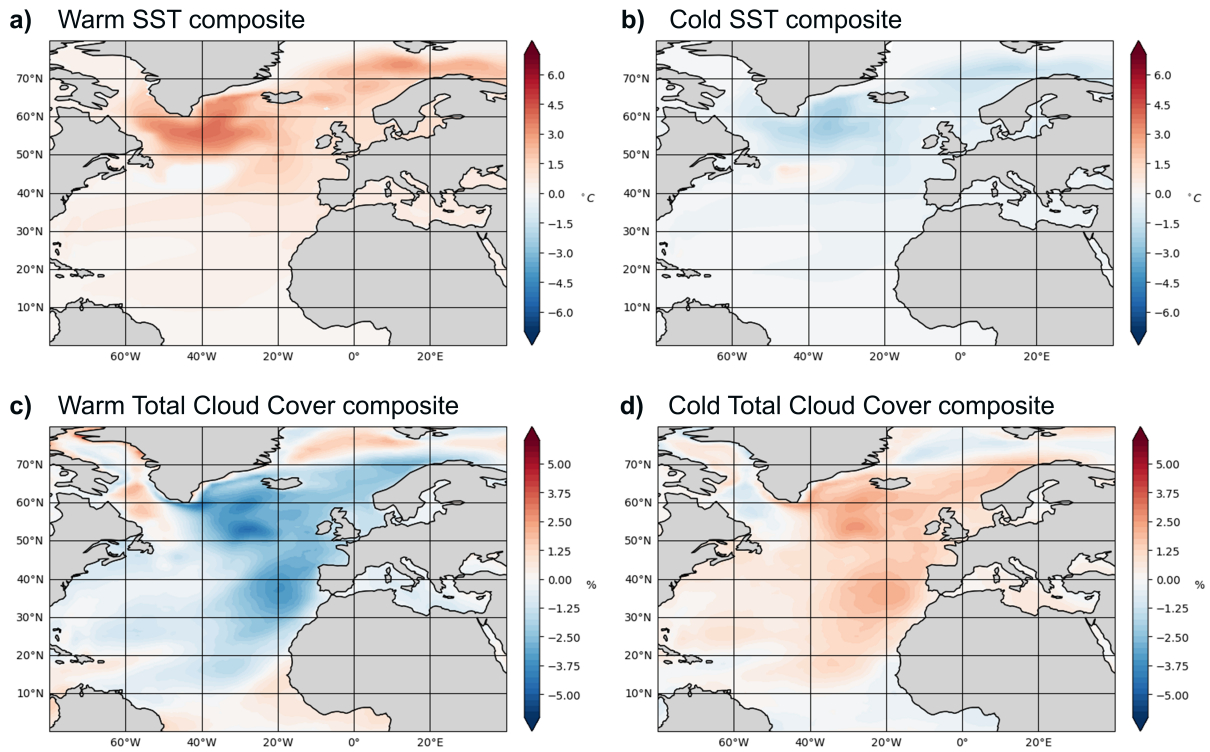
a Green's function approach. *Journal of Advances in Modeling Earth Systems*, *9*(5), 2174–2189. https://doi.org/10.1002/2017MS001096

Appendix

Figure A.1: Composites of SST ($°C$) during years experiencing a warm (a) AMV with one standard deviation above the mean of the whole AMV index, or cold (b) years falling one standard deviation below the mean. c) and d) are composites made in the same way with total cloud cover (%).
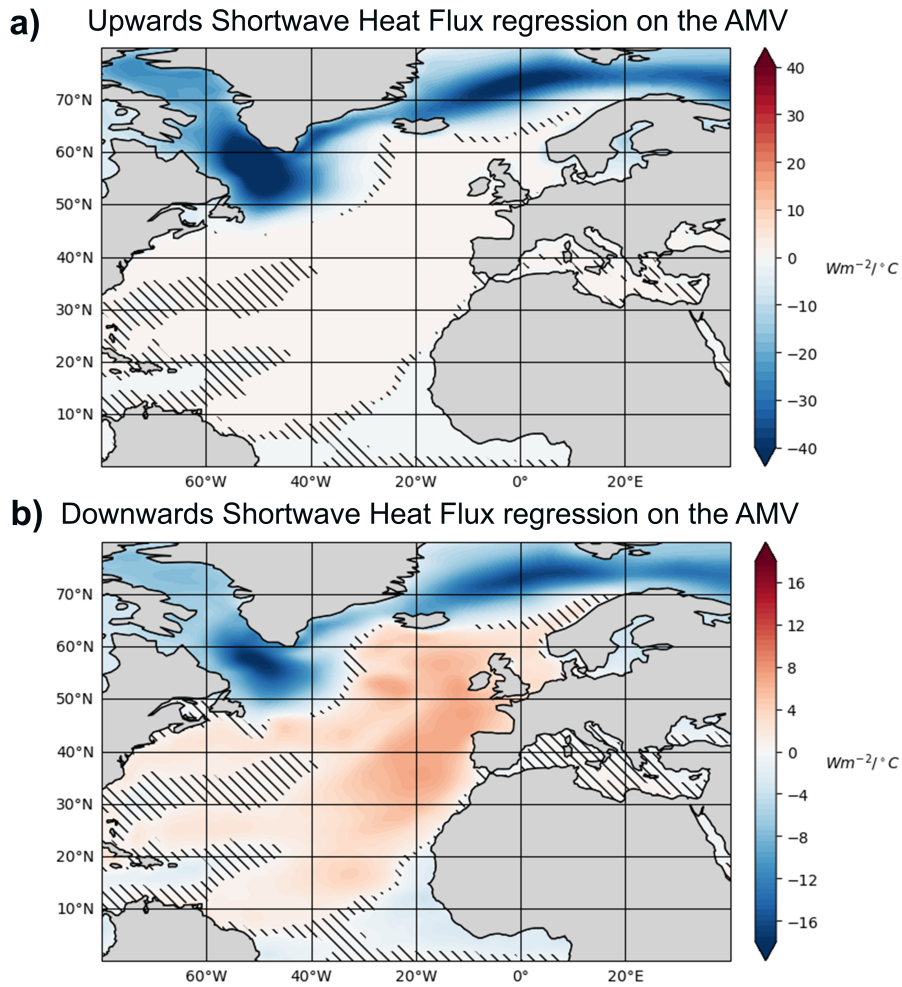
a) Upwards Shortwave Heat Flux regression on the AMV

b) Downwards Shortwave Heat Flux regression on the AMV

Figure A.2: Regression maps of shortwave heat flux against the AMV index in the North Atlantic. Positive (negative) values indicate an increase (decrease) in heat flux in units of Wm^{-2} per increase in $°C$ of the AMV index. 11-year running means have been applied to all the data. a) Shortwave heat flux directed upwards regressed on the observed AMV index. b) shortwave heat flux directed downwards regressed on the AMV index. Hatched bars indicate areas with non-statistically significant regions to the 99% level, as calculated according to Ebisuzaki (1997).
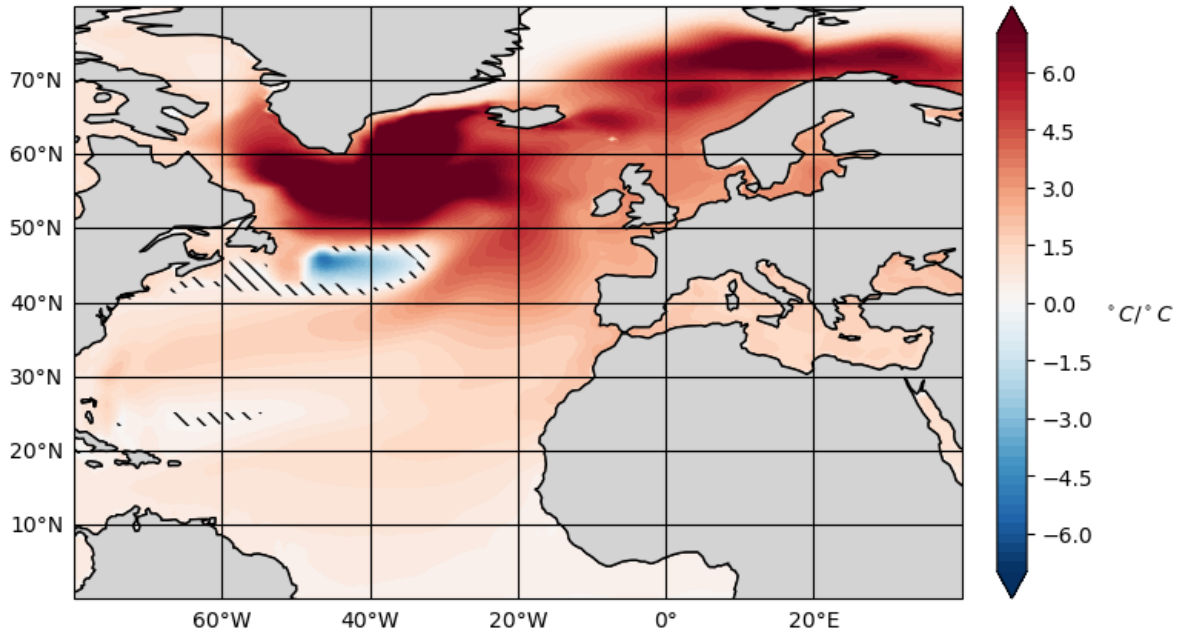
Figure A.3: Regression map of SST on the subtropical AMV index defined in the area between $7.5 - 75°W$ and $0 - 45°N$. The colorbar indicates changes in $°C$ in the North Atlantic per $°C$ increase in the subtropical AMV index. Hatched bars indicate areas with non-statistically significant regions to the 99% level, as calculated according to Ebisuzaki (1997).